

The Impact of Side Information on Physical Layer Security under Correlated Fading Channels

Farshad Rostami Ghadi, F. Javier López-Martínez, Wei-Ping Zhu, and Jean-Marie Gorce

Abstract—In this paper, we investigate the impact of side information (SI) on the performance of physical layer security (PLS) under correlated Rayleigh fading channels. By considering non-causally known SI at the transmitter and exploiting the copula technique to describe the fading correlation, we derived closed-form expressions for the average secrecy capacity (ASC) and secrecy outage probability (SOP) under positive/negative dependence conditions. We indicate that considering such knowledge at the transmitter is beneficial for system performance and ensures reliable communication with higher rates, as it improves the SOP and brings higher values of the ASC.

Index Terms—Physical layer security, side information, average secrecy capacity, secrecy outage probability, correlated fading.

I. INTRODUCTION

The broadcast nature and the inherent randomness of wireless channels have always made information security vulnerable to eavesdropping and jamming attacks. Therefore, the issues of reliability and security are momentous challenges in designing future wireless networks such as sixth-generation (6G) technology [1]–[3]. One of the alternative approaches to protect information from unauthorized access and guarantee secure communication instead of applying traditional cryptographic algorithms is physical layer security (PLS). The principle of PLS was first proposed by Shannon [4] and then studied by Wyner [5] for a basic wiretap channel exploiting Shannon’s notion of perfect secrecy. In Wyner’s proposed model, a transmitter wants to send a confidential message to a legitimate receiver through a discrete memoryless channel (DMC) while the eavesdropper attempts to decode the message. In this state, Wyner defined the maximum rate of reliable communication from the transmitter to the legitimate receiver as the secrecy capacity (SC), and showed that perfect secrecy could be achieved when the legitimate receiver has a better channel than the eavesdropper. Later, Csiszár and Körner extended Wyner’s result to non-degraded broadcast channels with confidential messages and showed that positive SC is always achievable if the main channel

(transmitter-to-legitimate receiver) is less noisy [6]. Leung-Yan-Cheong and Hellman also generalized Wyner’s studies to the Gaussian wiretap channel and defined the SC as the difference between capacities of the main and eavesdropper channels (transmitter-to-eavesdropper) [7]. On the other hand, due to the probable effects of the side information (SI) in reducing destructive effects of the interference and guaranteeing reliable communication with higher rates, Mitrpant *et al.* [8] analyzed the Gaussian wiretap channel with SI. Besides, by considering the Gaussian channel with known SI at the transmitter, Costa [9] described a dirty paper model in order to examine how much information can be reliably sent, assuming that the recipient cannot distinguish between ink and dirt. Costa’s analysis showed that the dirty channel model has the same capacity as the Gaussian model so that SI does not affect the channel capacity. Exploiting the similar approach of writing on dirty paper, Chen and Vink [10] studied the impact of SI on the Gaussian wiretap channel to find out how much secret information can be reliably and securely sent to the legitimate receiver without leaking information about the secret message to the eavesdropper. They showed that the SI at transmitter provides a larger SC and guarantees a more secure communication. Moreover, Chia and El Gamal [11] provided a lower bound of SC for the wiretap channel with SI available causally at both encoder and decoder, where they showed the lower bound in this case is strictly larger than that for the non-causal case obtained by Liu and Chen [12].

From the physical layer viewpoint, the received signal at the legitimate receiver and eavesdropper are different due to propagation environment effects such as large-scale and small-scale fading. Furthermore, the main channel and eavesdropper channel are practically correlated due to the physical limitation of antenna spacing or one physical environment, the proximity of the legitimate receiver and eavesdropper, and the presence or absence of scatters around them [13]. For this purpose, several works have analyzed secrecy metrics of PLS over various correlated fading *blank* (i.e., without SI) wiretap channels in recent years: The upper bound of SC and the asymptotic behavior of outage probability for a correlated Rayleigh fading wiretap channel were respectively studied in [14], [15]; closed-form expressions for the average secrecy capacity (ASC) and secrecy outage probability (SOP) over correlated Log-normal fading channels were obtained in [16]; SOP performance over correlated composite Nakagami- m /Gamma fading channels including shadowing and multi-path fading was investigated in [17]; compact expressions for the ASC and SOP in correlated $\alpha - \mu$ fading channels were derived in [18]. Moreover, only recently, the effect of fading correlation on the performance

Manuscript received xx, 2021; revised XXX. The review of this paper was coordinated by XXXX.

F.R. Ghadi and F.J. López Martínez are with Communications and Signal Processing Lab, Instituto Universitario de Investigación en Telecomunicación (TELMA), Universidad de Málaga, CEI Andalucía TECH, ETSI Telecomunicación, Bulevar Louis Pasteur 35, 29010 Málaga (Spain) (e-mail: farshad@ic.uma.es, fjlopezm@ic.uma.es).

W.P. Zhu is with Department of Electrical and Computer Engineering, Concordia University, Montreal, QC H3G 1M8, Canada (e-mail: weiping@ece.concordia.ca).

Jean-Marie Gorce is with the laboratoire CITI (a joint laboratory between the Université de Lyon, INRIA, and INSA de Lyon), 6 Avenue des Arts, F-69621, Villeurbanne, France (e-mail: jean - marie.gorce@inria.fr).

Digital Object Identifier 10.1109/XXX.2021.XXXXXXX

of PLS by exploiting copula theory was addressed in [19] and [20] again for the case of blank wiretap channels. Copula theory is a plausible approach to incorporate arbitrary dependence structures, that has recently become quite popular in the context of performance analysis of wireless communication systems [21]–[26]. In [19], the authors derived closed-form expressions for the ASC, SOP, and secrecy coverage region (SCR) over correlated Rayleigh fading channel using Farlie-Gumbel-Morgenstern (FGM) copula, while the authors in [20] represented the upper and lower bound of SOP for the same fading channel.

Motivated by the significant role of SI in providing a larger SC and rate equivocation region in wiretap channels, in this paper, we extend the dirty paper model of the Gaussian wiretap channel considered in [10], to wireless fading communications, in order to understand the behavior of important secrecy performance metrics under the assumption of SI at the transmitter. We also generalize [19] by considering a *correlated* wiretap fading channel and generate arbitrary multivariate coefficients of the main and eavesdropper channels by copula theory. Then, considering non-causally known SI at the transmitter under correlated Rayleigh fading wiretap channel, we exemplify how closed-form expressions for the ASC and SOP can be obtained for the case of using the FGM copula. The main contributions of our work are summarized as follows:

- We provide an information-theoretical copula-based formulation of the secure communication model over correlated wireless fading channels assuming non-causally SI at the transmitter and review the concept of copula theory and corresponding points.

- We represent a general formulation to describe the arbitrary dependence between fading channels coefficients and corresponding signal-to-noise ratios (SNRs). Then, by exploiting the compact probability density function (PDF) obtained by the FGM copula for Rayleigh fading coefficients, we derived the closed-form expression of ASC and SOP.

- Finally, we analyze the impact of non-causally known SI at the transmitter on the performance of ASC and SOP by changing the SI values and the dependence parameter within the defined range.

The rest of this paper is organized as follows. Section II describes the system model considered in our work. In section III, we characterize the SC of our proposed model. In section IV, we briefly review the concept of copula and provide the copula-based multivariate distribution, and then present the main results of secure communication with SI under correlated Rayleigh fading wiretap channel. We derive the exact closed-form expression of ASC and SOP in subsections V-A and V-B, respectively. In section VI, the validity of analytical results is illustrated numerically. Finally, the conclusions are drawn in section VII.

II. SYSTEM MODEL

We consider a wireless wiretap channel with the non-causally known SI S_i , $1 \leq i \leq n$ at the transmitter as shown in Fig. 1. In this scenario, the legitimate transmitter (Alice)

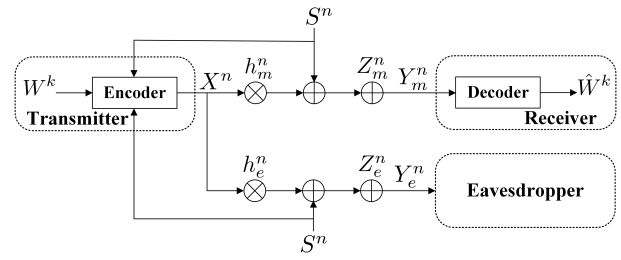


Fig. 1. System model depicting a correlated Rayleigh fading wiretap channel with SI at the transmitter.

sends the confidential message to the legitimate receiver (Bob) through the main channel (transmitter-to-receiver), while the eavesdropper (Eve) attempts to decode the message from its received signal through the eavesdropper channel (transmitter-to-eavesdropper). Let \mathcal{X}^n be the input set, \mathcal{Y}_m^n be the output set of the legitimate receiver, \mathcal{Y}_e^n be the output set of the eavesdropper, and \mathcal{S} be the finite set of SI at the transmitter. Specifically, we assume the transmitter wants to send a message $W^k \in \mathcal{W}^k = \{1, 2, \dots, M\}$ to the legitimate receiver in n uses of the channel. Since the SI is considered to be non-causally known at the transmitter, Alice encodes W^k and $S^n \in \mathcal{S}^n$ into a codeword $X^n \in \mathcal{X}^n$ for transmission over the main channel in a dirty paper fashion. Bob decodes the received signal $Y_m^n \in \mathcal{Y}_m^n$ by making an estimate $\hat{W}^k (Y_m^n)$ of the message W^k , while Eve received the signal $Y_e^n \in \mathcal{Y}_e^n$. Therefore, the received signals by Bob $Y_m(i)$ and by Eve $Y_e(i)$ can be determined as follows:

$$Y_m(i) = h_m(i)X(i) + S(i) + Z_m(i), \quad (1)$$

$$Y_e(i) = h_e(i)X(i) + S(i) + Z_e(i), \quad i = 1, \dots, n, \quad (2)$$

where $S(i)$ are the non-causally known SI at the transmitter, with variances Q ($S \sim \mathcal{N}(0, Q)$) which are independently and identically distributed (i.i.d) with probability distribution $p(s)$. The terms $Z_m(i)$ and $Z_e(i)$ correspond to i.i.d. additive white Gaussian noise (AWGN) with zero mean and variances N_m and N_e at the legitimate receiver and eavesdropper, respectively. Finally, $h_m(i)$ and $h_e(i)$ are the corresponding block fading channel Rayleigh coefficients and hence, the channel power gains are exponentially distributed (i.e., $g_m(i) = |h_m(i)|^2$ and $g_e(i) = |h_e(i)|^2$), where the fading process $h_m(i)$ and $h_e(i)$ are correlated. We suppose that both the main channel and eavesdropper channel are quasi-static fading channels, meaning that the fading coefficients, albeit random, are constant during the transmission of an entire codeword (i.e., $h_m(i) = h_m$ and $h_e(i) = h_e, \forall i = 1, \dots, n$) and independent from codeword to codeword. We also assume that the channel input, the channel fading coefficients, and the channel noises are all independent. Furthermore, we consider that the codewords sent by transmitter over the channels are subject to the average power constraint as follows:

$$\frac{1}{n} \sum_{i=1}^n \mathbb{E}\{|X(i)|^2\} \leq P. \quad (3)$$

Therefore, the instantaneous random SNR at the legitimate receiver and eavesdropper are given by $\gamma_m = \frac{P|h_m|^2}{N_m}$ and

$\gamma_e = \frac{P|h_e|^2}{N_e}$, respectively, while their corresponding average value are defined as $\bar{\gamma}_m = \frac{P\mathbb{E}\{|h_m|^2\}}{N_m}$ and $\bar{\gamma}_e = \frac{P\mathbb{E}\{|h_e|^2\}}{N_e}$. Besides, since the channel fading coefficients follow Rayleigh distribution, the corresponding random SNRs $\gamma_m > 0$ and $\gamma_e > 0$ are exponentially distributed with following marginal distributions: $f(\gamma_j) = \frac{1}{\bar{\gamma}_j}e^{-\frac{\gamma_j}{\bar{\gamma}_j}}$, $F(\gamma_j) = 1 - e^{-\frac{\gamma_j}{\bar{\gamma}_j}}$ for $j \in \{m, e\}$, respectively.

In the proposed system model, it is assumed that W^k is uniformly distributed on $\{1, 2, \dots, M\}$ as in 10. Thus, the transmission rate to the legitimate receiver is defined as $R = H(W^k)/n = \log M/n$, and the equivocation rate of the eavesdropper which indicates the secrecy level of confidential messages against the eavesdropper is denoted as $R_{eq} = H(W^k|Y_e^n)/n$, where $H(W^k|Y_e^n)$ is the remaining entropy of W^k conditioned on the value of Y_e^n . Besides, the average error probability is defined as:

$$\mathcal{P}_E = \frac{1}{M} \sum_{i=1}^M \Pr(\hat{W}^k(Y_m^n) \neq |W^k = i). \quad (4)$$

Consequently, the secrecy rate R_s is defined to be achievable, if there exist a code $(2^{nR_s}, n)$ such that for all $\epsilon > 0$ and sufficiently large n , $\mathcal{P}_E \leq \epsilon$ and $R_{eq} \geq R_s - \epsilon$. So, the SC \mathcal{C}_s can be defined as the supremum of achievable transmission rate R_s :

$$\mathcal{C}_s \triangleq \sup_{\mathcal{P}_E \leq \epsilon} R_s. \quad (5)$$

III. SECRECY CAPACITY DEFINITION

In this section, first, we introduce the SC definition for the discrete memoryless wiretap channel (DMWC) with SI at the transmitter. Then, we exploit this definition to derive the SC of the considered model in a wireless scenario.

Theorem 1. *The SC bounds for the DMWC with non-causally known SI at the transmitter was defined in [10] as follows:*

$$R_s^l \leq \mathcal{C}_s \leq R_s^u, \quad (6)$$

where

$$R_s^l = \max_{U \rightarrow (X, S) \rightarrow Y_m \rightarrow Y_e} I(U, Y_m) - \max\{I(U; S), I(U; Y_e)\}, \quad (7)$$

$$R_s^u = \min\{\mathcal{C}_m, \max_{U \rightarrow (X, S) \rightarrow Y_m \rightarrow Y_e} [I(U; Y_m) - I(U; Y_e)]\}, \quad (8)$$

U is a auxiliary random variable so that $U \rightarrow (X, S) \rightarrow Y_m \rightarrow Y_e$ forms a Markov chain, and \mathcal{C}_s is the capacity of the main channel with consideration of SI that is defined as:

$$\mathcal{C}_m = \max_{U \rightarrow (X, S) \rightarrow Y_m \rightarrow Y_e} [I(U; Y_m) - I(U; S)]. \quad (9)$$

Corollary 1. *According to Theorem 1, if there is an auxiliary parameter U_m so that*

- 1) $U_m \rightarrow (X, S) \rightarrow Y_m \rightarrow Y_e$ forms a Markov chain,
 - 2) $I(U_m; Y_m) - I(U_m; S) = \mathcal{C}_m$,
 - 3) $I(U_m; S) \geq I(U_m; Y_e)$,
- then the SC \mathcal{C}_s is equal to \mathcal{C}_m .

Corollary 2. *According to Theorem 1, if there is an auxiliary parameter U_e so that*

- 1) $U_e \rightarrow (X, S) \rightarrow Y_m \rightarrow Y_e$ forms a Markov chain,
 - 2) $I(U_e; Y_m) - I(U_e; Y_e) = R_e$,
 - 3) $I(U_e; Y_e) \geq I(U_e; S)$,
- then the SC \mathcal{C}_s is equal to R_e .

According to the conditions in Corollaries 1 and 2, the SC for a DMWC could be \mathcal{C}_m or R_e . Now, by extending Theorem 1 to the Gaussian wiretap channel and assuming the auxiliary random variable $U = X + \alpha S$, where α is a real number and X is independent of S , the SC can be determined. To this end, the following lemma is considered to specify the range of parameter α and determine the conditions of Corollaries 1 and 2.

Lemma 1. *The conditions for Corollaries 1 and 2 are explicitly realized based on the system model parameters as:*

$$I(U; S) \geq I(U; Y_e) \iff \alpha \geq \alpha_0 \text{ or } \alpha \leq \alpha_{-0}, \quad (10)$$

$$I(U; S) < I(U; Y_e) \iff \alpha_{-0} < \alpha < \alpha_0, \quad (11)$$

where

$$\alpha_0 = \frac{P}{P + N_e} \left(1 + \sqrt{\frac{P + Q + N_e}{N_e}} \right), \quad (12)$$

$$\alpha_{-0} = \frac{P}{P + N_e} \left(1 - \sqrt{\frac{P + Q + N_e}{N_e}} \right). \quad (13)$$

Proof. The details of the proof are in Appendix A. \square

Here, by considering Lemma 1 and Corollaries 1 and 2, SC for the block fading wiretap channel with non-causally known SI at the transmitter is defined as the following theorem.

Theorem 2. *The SC \mathcal{C}_s for the block fading wiretap channel with non-causally known SI at the transmitter is determined as:*

$$\mathcal{C}_s = \begin{cases} \log_2(1 + \gamma_m), & \text{if Corollary 1} \\ \log_2\left(\frac{1 + \bar{\gamma}_{ms} + \gamma_m}{1 + \bar{\gamma}_{es} + \gamma_e}\right), & \text{if Corollary 2} \end{cases}, \quad (14)$$

where $\bar{\gamma}_{ms} = \frac{Q}{N_m}$ and $\bar{\gamma}_{es} = \frac{Q}{N_e}$.

Proof. The details of the proof are in Appendix B. \square

IV. COPULA-BASED MULTIVARIATE DISTRIBUTION

Since the fading channel coefficients are assumed correlated in the considered model, we need to generate the corresponding multivariate distribution of the random SNRs. Therefore, in this section, we first briefly review the concept of copula theory [27], and then we determine the joint PDF of the main channel and eavesdropper SNRs. As mentioned in the literature, copula theory is a flexible approach to generate the multivariate distribution of correlated random variables (RVs) by only using their corresponding marginal distributions. Besides, copulas are defined by a particular dependence parameter which indicates the intensity of dependency for unknown RVs.

Definition 1 (Two-dimensional copula). *Let $\mathbf{V} = (V_1, V_2)$ be a vector of two RVs with marginal cumulative distribution*

functions (CDFs) $F(v_b) = \Pr(V_b \leq v_b)$ for $b = 1, 2$, respectively, and relevant bivariate CDF $F(v_1, v_2) = \Pr(V_1 \leq v_1, V_2 \leq v_2)$. Then, the copula function $C(u_1, u_2)$ of $\mathbf{V} = (V_1, V_2)$ defined on the unit hypercube $[0, 1]^2$ with uniformly distributed RVs $U_b := F(v_b)$ for $b = 1, 2$ over $[0, 1]$ is given by

$$C(u_1, u_2) = \Pr(U_1 \leq u_1, U_2 \leq u_2). \quad (15)$$

Theorem 3 (Sklar's theorem). *Let $F(v_1, v_2)$ be a joint CDF of RVs with margins $F(v_b)$ for $b = 1, 2$. Then, there exists one copula function C such that for all v_b in the extended real line domain \bar{R} ,*

$$F(v_1, v_2) = C(F(v_1), F(v_2)). \quad (16)$$

Corollary 3. *By applying the chain rule to (16), the joint PDF $f(v_1, v_2)$ is derived as:*

$$f(v_1, v_2) = f(v_1)f(v_2)c(F(v_1), F(v_2)), \quad (17)$$

where $c(F(v_1), F(v_2)) = \frac{\partial^2 C(F(v_1), F(v_2))}{\partial F(v_1) \partial F(v_2)}$ is the copula density function and $f(v_b)$ for $b = 1, 2$ are the marginal PDFs, respectively.

Theorem 4 (Fréchet-Hoeffding bounds). *For any copula function $C : [0, 1]^2 \rightarrow [0, 1]$ and any $(u_1, u_2) \in [0, 1]^2$, the following bounds hold: $C^- \prec C \prec C^+$; where $C_1 \prec C_2$ if $C_1(u_1, u_2) \leq C_2(u_1, u_2) \forall (u_1, u_2) \in [0, 1]^2$, and*

$$C^-(u_1, u_2) = \max(u_1 + u_2 - 1, 0), \quad (18)$$

$$C^+(u_1, u_2) = \min(u_1, u_2). \quad (19)$$

The upper and lower bounds model extreme dependence structures. If $C = C^-$ the pair of RVs are said to be countermonotonic, whereas $C = C^+$ means that both RVs are comonotonic. The copula function for the independent case $C^\perp(u_1, u_2) = u_1 u_2$ defines the limit between positive and negative dependence. Let us assume two Copulas that verify: $C^- \prec C_1 \prec C^\perp \prec C_2 \prec C^+$. Then, C_1 models a negative dependence and C_2 a positive dependence.

The above definitions are valid for any arbitrary choice of copula. We will now indicate how the secrecy performance metrics can be characterized in the closed-form expression for FGM copula. This selection is justified because it can describe both positive and negative dependences between RVs, while offering good mathematical tractability.

Definition 2. [FGM copula] *The FGM copula with dependence parameter $\theta \in [-1, 1]$ is defined as:*

$$C_F(u_1, u_2) = u_1 u_2 (1 + \theta(1 - u_1)(1 - u_2)), \quad (20)$$

where $\theta \in [-1, 0)$ and $\theta \in (0, 1]$ denote the negative and positive dependence structures respectively, while $\theta = 0$ indicates the independence structure.

Lemma 2. *The joint PDF of γ_m and γ_e based on FGM copula is determined as:*

$$f(\gamma_m, \gamma_e) = \frac{e^{-\frac{\gamma_m}{\bar{\gamma}_m} - \frac{\gamma_e}{\bar{\gamma}_e}}}{\bar{\gamma}_m \bar{\gamma}_e} \left[1 + \theta \left(1 - 2e^{-\frac{\gamma_m}{\bar{\gamma}_m}} \right) \left(1 - 2e^{-\frac{\gamma_e}{\bar{\gamma}_e}} \right) \right]. \quad (21)$$

Proof. By applying the partial derivatives in (20), inserting it into (17), and then considering the SNRs marginal distribution, the proof is completed. \square

V. SECRECY PERFORMANCE METRICS: ASC AND SOP

In this section, we derive closed-form expressions for ASC and SOP by exploiting the joint PDF obtained in section IV.

A. ASC Analysis

The ASC for considered system model based on Corollaries 1 and 2 can be defined as:

$$\bar{C}_s^1 = \int_0^\infty \int_0^\infty \log_2(1 + \gamma_m) f(\gamma_m, \gamma_e) d\gamma_e d\gamma_m, \quad (22)$$

$$\bar{C}_s^2 = \int_0^\infty \int_0^{\bar{\gamma}} \log_2\left(\frac{1 + \bar{\gamma}_{ms} + \gamma_m}{1 + \bar{\gamma}_{es} + \gamma_e}\right) f(\gamma_m, \gamma_e) d\gamma_e d\gamma_m, \quad (23)$$

where $\bar{\gamma} = \gamma_m + \bar{\gamma}_{ms} - \bar{\gamma}_{es}$.

Theorem 5. *The ASC for concerned correlated Rayleigh fading wiretap channel with non-causally known SI at the transmitter under consideration of the Corollary 1 and Corollary 2 is determined as:*

$$\bar{C}_s = \begin{cases} \bar{C}_s^1, & \text{if Corollary 1} \\ \bar{C}_s^2, & \text{if Corollary 2} \end{cases}, \quad (24)$$

where \bar{C}_s^1 and \bar{C}_s^2 are given by (25) and (26), respectively; and $E_1(t) = \int_t^\infty \frac{e^{-z}}{z} dz$ is the Exponential Integral.

Proof. The details of the proof are in Appendix C. \square

B. SOP Analysis

The SOP is defined as the probability that the random SC \mathcal{C}_s is less than a target secrecy rate $R_s > 0$, or:

$$P_{sop} = \Pr(\mathcal{C}_s \leq R_s) = 1 - \Pr(\mathcal{C}_s > R_s). \quad (27)$$

So, the SOP under consideration of Corollary 1 is defined as:

$$P_{sop}^1 = 1 - \Pr(\log_2(1 + \gamma_m) > R_s) \quad (28)$$

$$= 1 - \Pr(\gamma_m > 2^{R_s} - 1) \quad (29)$$

$$= 1 - \int_0^\infty \int_{2^{R_s}-1}^\infty f(\gamma_m, \gamma_e) d\gamma_m d\gamma_e, \quad (30)$$

and similarly, the SOP under consideration of Corollary 2 is given by

$$P_{sop}^2 = 1 - \Pr\left(\log\left(\frac{1 + \bar{\gamma}_{ms} + \gamma_m}{1 + \bar{\gamma}_{es} + \gamma_e}\right) > R_s\right) \quad (31)$$

$$= 1 - \Pr(\gamma_m > 2^{R_s} (1 + \bar{\gamma}_{es} + \gamma_e) - (1 + \bar{\gamma}_{ms})) \quad (32)$$

$$= 1 - \int_0^\infty \int_{\gamma_{th}}^\infty f(\gamma_m, \gamma_e) d\gamma_m d\gamma_e, \quad (33)$$

where $\gamma_{th} = 2^{R_s} (1 + \bar{\gamma}_{es} + \gamma_e) - (1 + \bar{\gamma}_{ms})$.

Theorem 6. *The SOP for concerned correlated Rayleigh fading wiretap channel with non-causally known SI at the transmitter under consideration of the Corollary 1 and Corollary 2 is given by*

$$P_{sop} = \begin{cases} P_{sop}^1, & \text{if Corollary 1} \\ P_{sop}^2, & \text{if Corollary 2} \end{cases}, \quad (34)$$

$$\bar{C}_s^1 = \frac{e^{\frac{1}{\bar{\gamma}_m}}}{\ln 2} E_1 \left(\frac{1}{\bar{\gamma}_m} \right), \quad (25)$$

$$\begin{aligned} \bar{C}_s^2 = & \frac{1}{\ln 2} \left(\ln \left(\frac{1 + \bar{\gamma}_{ms}}{1 + \bar{\gamma}_{es}} \right) + e^{\frac{1 + \bar{\gamma}_{ms}}{\bar{\gamma}_m}} E_1 \left(\frac{1 + \bar{\gamma}_{ms}}{\bar{\gamma}_m} \right) - e^{\frac{1 + \bar{\gamma}_{es}}{\bar{\gamma}_e}} \left(E_1 \left(\frac{1 + \bar{\gamma}_{ms}}{\bar{\gamma}_e} \right) - E_1 \left(\frac{1 + \bar{\gamma}_{es}}{\bar{\gamma}_e} \right) \right) \right. \\ & - e^{\frac{1 + \bar{\gamma}_{es}}{\bar{\gamma}_e} + \frac{1 + \bar{\gamma}_{ms}}{\bar{\gamma}_m}} \left(E_1 \left(\frac{(\bar{\gamma}_m + \bar{\gamma}_e)(1 + \bar{\gamma}_{ms})}{\bar{\gamma}_m \bar{\gamma}_e} \right) + \theta \left[E_1 \left(\frac{(\bar{\gamma}_m + \bar{\gamma}_e)(1 + \bar{\gamma}_{ms})}{\bar{\gamma}_m \bar{\gamma}_e} \right) - e^{\frac{(1 + \bar{\gamma}_{ms})}{\bar{\gamma}_m}} E_1 \left(\frac{(\bar{\gamma}_m + 2\bar{\gamma}_e)(1 + \bar{\gamma}_{ms})}{\bar{\gamma}_m \bar{\gamma}_e} \right) \right. \right. \\ & \left. \left. - e^{\frac{(1 + \bar{\gamma}_{es})}{\bar{\gamma}_e}} E_1 \left(\frac{(2\bar{\gamma}_m + \bar{\gamma}_e)(1 + \bar{\gamma}_{ms})}{\bar{\gamma}_m \bar{\gamma}_e} \right) + e^{\frac{(1 + \bar{\gamma}_{es})}{\bar{\gamma}_e} + \frac{(1 + \bar{\gamma}_{ms})}{\bar{\gamma}_m}} E_1 \left(\frac{(2\bar{\gamma}_m + \bar{\gamma}_e)(1 + \bar{\gamma}_{ms})}{\bar{\gamma}_m \bar{\gamma}_e} \right) \right] \right). \quad (26) \end{aligned}$$

where P_{sop}^1 and P_{sop}^2 are expressed as follows:

$$P_{sop}^1 = 1 - e^{-\frac{(2R_s - 1)}{\bar{\gamma}_m}}, \quad (35)$$

$$\begin{aligned} P_{sop}^2 = & 1 - \left[\frac{\bar{\gamma}_m e^{-\frac{\bar{\gamma}_{th}}{\bar{\gamma}_m}}}{\bar{\gamma}_m + 2R_s \bar{\gamma}_e} + \theta \left(\frac{\bar{\gamma}_m e^{-\frac{\bar{\gamma}_{th}}{\bar{\gamma}_m}}}{\bar{\gamma}_m + 2R_s \bar{\gamma}_e} - \frac{\bar{\gamma}_m e^{-\frac{2\bar{\gamma}_{th}}{\bar{\gamma}_m}}}{\bar{\gamma}_m + 2R_s + 1 \bar{\gamma}_e} \right. \right. \\ & \left. \left. - \frac{2\bar{\gamma}_m e^{-\frac{\bar{\gamma}_{th}}{\bar{\gamma}_m}}}{2\bar{\gamma}_m + 2R_s \bar{\gamma}_e} + \frac{\bar{\gamma}_m e^{-\frac{2\bar{\gamma}_{th}}{\bar{\gamma}_m}}}{\bar{\gamma}_m + 2R_s \bar{\gamma}_e} \right) \right], \quad (36) \end{aligned}$$

and $\bar{\gamma}_{th} = 2R_s (1 + \bar{\gamma}_{es}) - (1 + \bar{\gamma}_{ms})$.

Proof. The details of proof are in Appendix D. \square

VI. NUMERICAL RESULTS

In this section, the analytical expressions previously derived and Monte-Carlo (MC) simulation for the ASC and SOP are presented, with the special focus on comparing the performances in the presence/absence of SI and fading correlation. It should be noted that for the case of analyzing ASC under correlated fading, additional simulations are included using the Frank copula [27] to extend the analytical results obtained with the FGM copula to a wider range of values for both positive and negative dependencies by exploiting Frank's copula parameter $\zeta \in \mathbb{R} \setminus \{0\}$.

Fig. 2 shows the impact of SI on the performance of ASC \bar{C}_s based on the variations of the average main channel SNR $\bar{\gamma}_m$ for selected values of the average eavesdropper channel SNR $\bar{\gamma}_e$ and given values of SI under positive dependence structure. It can be seen that SI does not affect the performance of the ASC under consideration of Corollary 1 since \bar{C}_s^1 is independent of SI and only depends on $\bar{\gamma}_m$ based on SC definition in (14). On the other hand, it is observed that the SI has positive effects on the behavior of the ASC under Corollary 2, so that for the low SNR regime the efficiency of SI is more tangible as compared with the high SNR regime. To further evaluate the impact of SI, the behavior of ASC based on the SI ratio (i.e., $\bar{\gamma}_{ms}/\bar{\gamma}_{es}$) for three different scenarios $\bar{\gamma}_m > \bar{\gamma}_e$, $\bar{\gamma}_m = \bar{\gamma}_e$, and $\bar{\gamma}_m < \bar{\gamma}_e$ under positive dependence structure is illustrated in Fig. 3. It is clear that for all three scenarios, \bar{C}_s^1 is constant during the changes of the SI ratio and only depends on the values of $\bar{\gamma}_m$. On the other side, \bar{C}_s^2 continuously increases by increasing the SI ratio for all

scenarios. The interesting point is that even under the condition that the main channel is worse than the eavesdropper channel (i.e., $\bar{\gamma}_m < \bar{\gamma}_e$), \bar{C}_s^2 still grows and the ASC is achievable. In Fig. 4, the effect of SI on the performance of SOP based on the variations of $\bar{\gamma}_m$ for selected values of $\bar{\gamma}_e$ and given values of SI under positive dependence structure is provided. It can be seen that P_{sop}^1 provides the lowest values of SOP and it is independent of the SI and $\bar{\gamma}_e$. In contrast, considering SI at the transmitter has constructive effects on the performance of P_{sop}^2 so that for all selected values of $\bar{\gamma}_e$, a lower value of SOP is achievable as compared to the case where there is no SI.

From a correlation viewpoint, we evaluate the impact of fading correlation on the performance of ASC and SOP in the presence of SI in Figs. 5 and 6. In these cases, we have modeled the correlated fading channels based on the copula approach where the dependence parameter shows the measure of dependency. In this regard, it should be noted there is a relation between the linear correlation coefficient $\rho \triangleq \text{cov}[\gamma_m \gamma_e] / \sqrt{\text{var}[\gamma_m] \text{var}[\gamma_e]}$ and the copula dependence parameter. Therefore, to have a clearer insight with conventional correlation, we also approximate the corresponding values of ρ for the considered copula dependence parameters. Fig. 5 shows the behavior of ASC in terms of $\bar{\gamma}_m$ under correlated Rayleigh fading channels for selected values of the dependence parameters and SI. Given the independence of \bar{C}_s^1 from correlation and SI, it is clear that \bar{C}_s^1 gains higher values in terms of ASC during the changes of $\bar{\gamma}_m$. In contrast, it can be observed that the correlation effect is gradually eliminated in the high SNR regime in terms of P_{sop}^2 . We also see that positive dependence worsens the ASC performance compared to the independent fading case since as the channels become more correlated, they tend to behave more similarly, and thus the chances for the transmitter to transmit at a high secrecy rate decreases. It should be noted that the Fréchet-Hoeffding bounds are not symmetric w.r.t. $\rho = 0$, but they tend to ± 1 . Therefore, we observe that the Frank copula gets close to the Fréchet-Hoeffding bounds for $\zeta = \pm 35$ in Fig. 5, which exhibits a non-symmetric behavior. We also see that correlation for the case with FGM copula is now symmetric since such copula only can model weak dependences, and hence is distant to the Fréchet-Hoeffding bounds, thus not reaching the maximum permissible range of ± 1 for ρ .

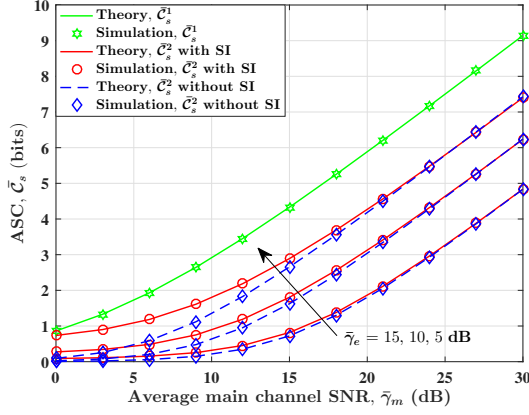


Fig. 2. The ASC versus $\bar{\gamma}_m$ for selected values of $\bar{\gamma}_e$, a target secrecy rate $R_s = 1.5$ bits, the FGM dependence parameter $\theta = 1$, and given values of SI $\bar{\gamma}_{ms} = 5$ dB, $\bar{\gamma}_{es} = -10$ dB.

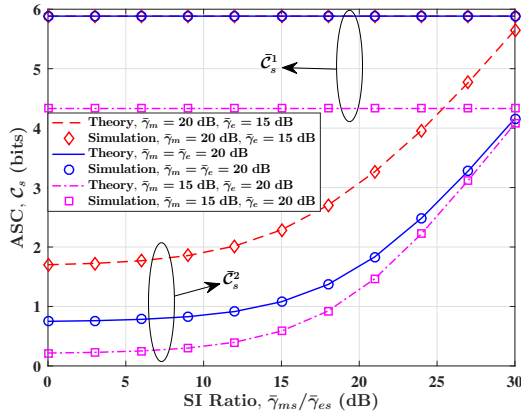


Fig. 3. The ASC versus $\bar{\gamma}_{ms}/\bar{\gamma}_{es}$ for a target secrecy rate $R_s = 1.5$ bits, the FGM dependence parameter $\theta = 1$, and different scenarios when, (a) the main channel's condition is better than the eavesdropper's ($\bar{\gamma}_m > \bar{\gamma}_e$), (b) the main channel's condition is the same as eavesdropper's ($\bar{\gamma}_m = \bar{\gamma}_e$), and (c) the main channel's condition is worse than the eavesdropper's ($\bar{\gamma}_m < \bar{\gamma}_e$).

In Fig. 6 the performance of SOP in terms of $\bar{\gamma}_m$ under correlated Rayleigh fading channels for selected values of dependence parameters and SI is represented. As expected, P_{sop}^1 provides the lowest values of SOP during $\bar{\gamma}_m$ variations regardless the correlation effects. In contrast, it can be seen that when the main channel is better than the eavesdropper channel ($\bar{\gamma}_m > \bar{\gamma}_e$), P_{sop}^2 will be achieved less than 0.5, while under the condition that $\bar{\gamma}_m \leq \bar{\gamma}_e$, P_{sop}^2 becomes greater than 0.5. In this case, we can see that the positive dependence improves the SOP performance as compared with the independent fading case when $P_{sop}^2 < 0.5$, since if $\bar{\gamma}_m > \bar{\gamma}_e$, then the larger the correlation level, the higher the probability of having $\gamma_m > \gamma_e$.

VII. CONCLUSION

In this paper, we analyzed the impact of SI on PLS performance under correlated fading channels. To this end, we derived the closed-form expressions for ASC and SOP by exploiting copula theory in the presence of SI and fading correlation. We proved that considering the SI at the transmitter,

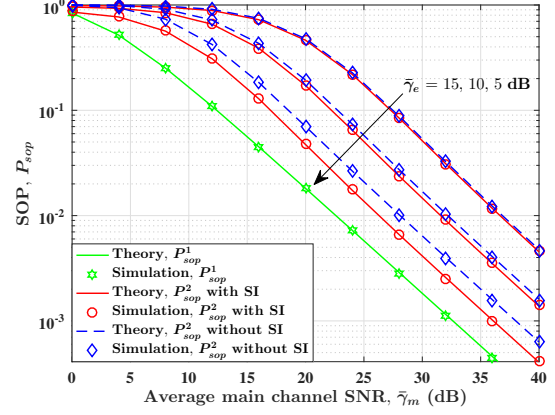


Fig. 4. The SOP versus $\bar{\gamma}_m$ for selected values of $\bar{\gamma}_e$, a target secrecy rate $R_s = 1.5$ bits, the FGM dependence parameter $\theta = 1$, and given values of SI $\bar{\gamma}_{ms} = 5$ dB, $\bar{\gamma}_{es} = -5$ dB.

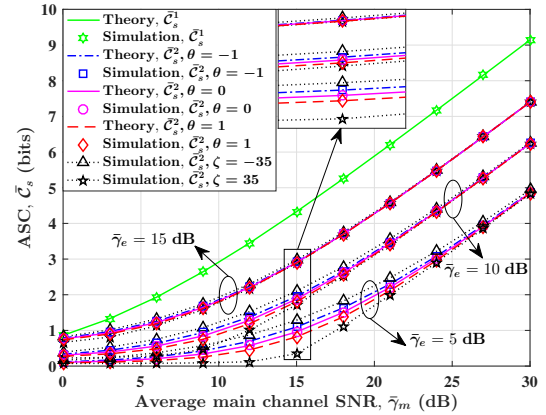


Fig. 5. The ASC versus $\bar{\gamma}_m$ for selected values of $\bar{\gamma}_e$, a target secrecy rate $R_s = 1.5$ bits, the FGM dependence parameter $\theta = \pm 1$ ($\rho \approx \pm 0.25$), $\zeta = \pm 35$ ($\rho \approx [-0.63, 0.92]$) and given values of SI $\bar{\gamma}_{ms} = 5$ dB, $\bar{\gamma}_{es} = -10$ dB.

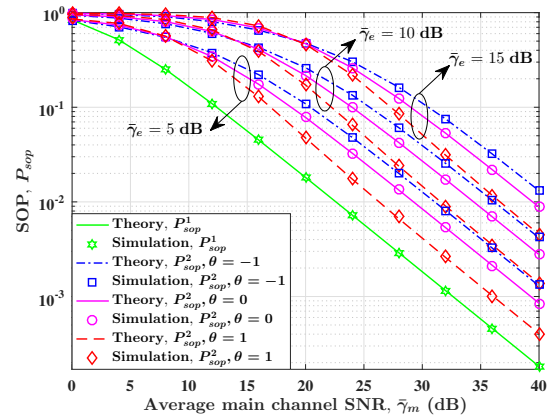


Fig. 6. The SOP versus $\bar{\gamma}_m$ for selected values of $\bar{\gamma}_e$, a target secrecy rate $R_s = 1.5$ bits, the FGM dependence parameter $\theta = \pm 1$ ($\rho \approx \pm 0.25$), $\zeta = \pm 35$ ($\rho \approx [-0.63, 0.92]$) and given values of SI $\bar{\gamma}_{ms} = 5$ dB, $\bar{\gamma}_{es} = -5$ dB.

compared with the *blank* fading wiretap channel considered in [19], improves the efficiency of the system model in terms

of ASC and SOP. Hence, an increase in SI provides a higher value of ASC as well as a lower SOP. We also showed that for a fixed SI, an increment in the correlation decreases the ASC in the low SNR regime, while improves the performance of SOP in the specific cases.

APPENDIX A PROOF OF LEMMA 1

By considering the Gaussian case, we compute the values of mutual information $I(U; S)$ and $I(U; Y_e)$ as follows:

$$I(U; S) = I(X + \alpha S; S) \quad (37)$$

$$= H(X + \alpha S) + H(S) - H(X + \alpha S, S) \quad (38)$$

$$= \log \left((2\pi e)^2 (P + \alpha^2 Q) Q \right) - \log \left((2\pi e)^2 ((P + \alpha^2 Q) Q - \alpha^2 Q^2) \right) \quad (39)$$

$$= \log \left(\frac{P + \alpha^2 Q}{P} \right). \quad (40)$$

and

$$I(U; Y_e) = I(X + \alpha S; X + S + Z_e) \quad (41)$$

$$= H(X + S + Z_e) - H(X + S + Z_e | X + \alpha S) \quad (42)$$

$$= H(X + S + Z_e) + H(X + \alpha S) - H(X + S + Z_e, X + \alpha S) \quad (43)$$

$$= \log \left((2\pi e)^2 (P + Q + N_e) (P + \alpha^2 Q) \right) - \log \left((2\pi e)^2 \det(\text{cov}(X + S + Z_e, X + \alpha S)) \right) \quad (44)$$

$$= \log \left(\frac{(P + Q + N_e) (P + \alpha^2 Q)}{PQ(1 - \alpha)^2 + N_e(P + \alpha^2 Q)} \right). \quad (45)$$

Now we consider the inequality $I(U; S) \geq I(U; Y_e)$, and we have:

$$I(U; S) \geq I(U; Y_e) \quad (46)$$

$$\log \left(\frac{P + \alpha^2 Q}{P} \right) \geq \log \left(\frac{(P + Q + N_e) (P + \alpha^2 Q)}{PQ(1 - \alpha)^2 + N_e(P + \alpha^2 Q)} \right) \quad (47)$$

$$\frac{1}{P} > \frac{(P + Q + N_e)}{PQ(1 - \alpha)^2 + N_e(P + \alpha^2 Q)} \quad (48)$$

$$\alpha^2 Q(P + N_e) - 2PQ\alpha - P^2 > 0. \quad (49)$$

Therefore, $\alpha \geq \frac{P}{P+N_e} \left(1 + \sqrt{\frac{P+Q+N_e}{N_e}} \right) = \alpha_0$ or $\alpha \leq \frac{P}{P+N_e} \left(1 - \sqrt{\frac{P+Q+N_e}{N_e}} \right) = \alpha_{-0}$. Similarly, for inequality $I(U; S) < I(U; Y_e)$ we have: $\frac{P}{P+N_e} \left(1 - \sqrt{\frac{P+Q+N_e}{N_e}} \right) = \alpha_{-0} < \alpha < \frac{P}{P+N_e} \left(1 + \sqrt{\frac{P+Q+N_e}{N_e}} \right) = \alpha_0$.

APPENDIX B PROOF OF THEOREM 2

Here, exploiting the same coding method used in [10]–[12] to achieve the SC, we prove Theorem 2 considering the known fading coefficients h_m and h_e . To this end, we assume $U_m = X + \alpha_m S$ and $U_e = X + \alpha_e S$ as used for generalized

dirty paper coding [9], where X and S are independent RVs distributed according to $\mathcal{N}(0, P)$ and $\mathcal{N}(0, Q)$, respectively, and α_m and α_e are parameters to be later determined. So, by considering (1), we compute the values of mutual information $I(U_m; Y_m)$ and $I(U_m; S)$ as follows:

$$I(U_m; Y_m) = I(X + \alpha_m S; h_m X + S + Z_m) \quad (50)$$

$$= H(h_m X + S + Z_m) - H(h_m X + S + Z_m | X + \alpha_m S) \quad (51)$$

$$= H(h_m X + S + Z_m) + H(X + \alpha_m S) - H(h_m X + S + Z_m, X + \alpha_m S) \quad (52)$$

$$= \log \left((2\pi e)^2 (|h_m|^2 P + Q + N_m) (P + \alpha_m^2 Q) \right) - \log \left((2\pi e)^2 \det(\text{cov}(h_m X + S + Z_m, X + \alpha_m S)) \right) \quad (53)$$

$$= \log \left(\frac{(|h_m|^2 P + Q + N_m) (P + \alpha_m^2 Q)}{PQ(1 - |h_m|\alpha_m)^2 + N_m(P + \alpha_m^2 Q)} \right), \quad (54)$$

and

$$I(U_m; S) = I(X + \alpha_m S; S) \quad (55)$$

$$= H(X + \alpha_m S) + H(S) - H(X + \alpha_m S, S) \quad (56)$$

$$= \log \left((2\pi e)^2 (P + \alpha_m^2 Q) Q \right) - \log \left((2\pi e)^2 ((P + \alpha_m^2 Q) Q - \alpha_m^2 Q^2) \right) \quad (57)$$

$$= \log \left(\frac{P + \alpha_m^2 Q}{P} \right). \quad (58)$$

Now, by inserting (54) and (58) into \mathcal{C}_s defined in Corollary 1, we have:

$$\mathcal{C}_m(\alpha_m) = \log \left(\frac{P(|h_m|^2 P + Q + N_m)}{PQ(1 - |h_m|\alpha_m)^2 + N_m(P + \alpha_m^2 Q)} \right). \quad (59)$$

Consequently, by maximizing $\mathcal{C}_m(\alpha_m)$ over α_m , the SC \mathcal{C}_s can be obtained as:

$$\mathcal{C}_s = \max_{\alpha_m} \mathcal{C}_m(\alpha_m) \quad (60)$$

$$= \log \left(1 + \frac{|h_m|^2 P}{N_m} \right) \quad (61)$$

$$= \log(1 + \gamma_m). \quad (62)$$

In order to prove the SC \mathcal{C}_s for the second condition, we need to calculate the values of mutual information $I(U_e; Y_m)$ and $I(U_e; Y_e)$. Similarly, by considering (2) and $U_e = X + \alpha_e S$, we have:

$$I(U_e; Y_m) = \log \left(\frac{(|h_m|^2 P + Q + N_m) (P + \alpha_e^2 Q)}{PQ(1 - |h_m|\alpha_e)^2 + N_m(P + \alpha_e^2 Q)} \right), \quad (63)$$

and

$$I(U_e; Y_e) = \log \left(\frac{(|h_e|^2 P + Q + N_e) (P + \alpha_e^2 Q)}{PQ(1 - |h_e|\alpha_e)^2 + N_e(P + \alpha_e^2 Q)} \right). \quad (64)$$

Now, by substituting (63) and (64) in \mathcal{C}_s defined in Corollary 2, we obtain:

$$R_e(\alpha_e) = \log \left(\frac{(|h_m|^2 P + Q + N_m) (PQ(1 - |h_e|\alpha_e)^2 + N_e(P + \alpha_e^2 Q))}{(|h_e|^2 P + Q + N_e) (PQ(1 - |h_m|\alpha_e)^2 + N_m(P + \alpha_e^2 Q))} \right). \quad (65)$$

Finally, by maximizing $R_e(\alpha_e)$ over α_e , the SC \mathcal{C}_s can be determined as:

$$\mathcal{C}_s = \max_{\alpha_e} R_e(\alpha_e) = \log \left(\frac{1 + \bar{\gamma}_{ms} + \gamma_m}{1 + \bar{\gamma}_{es} + \gamma_e} \right). \quad (66)$$

APPENDIX C PROOF OF THEOREM 5

Proof of $\bar{\mathcal{C}}_s^1$: By substituting the joint PDF $f(\gamma_m, \gamma_e)$ in to (22), the ASC under condition of the Corollary 1 can be determined as:

$$\bar{\mathcal{C}}_s^1 = \frac{1}{\bar{\gamma}_m \bar{\gamma}_e} \int_0^\infty \int_0^{\bar{\gamma}} \log_2(1 + \gamma_m) e^{-\frac{\gamma_m}{\bar{\gamma}_m} - \frac{\gamma_e}{\bar{\gamma}_e}} \times \left[1 + \theta(1 - 2e^{-\frac{\gamma_m}{\bar{\gamma}_m}})(1 - 2e^{-\frac{\gamma_e}{\bar{\gamma}_e}}) \right] d\gamma_e d\gamma_m \quad (67)$$

$$\begin{aligned} &= \frac{1}{\bar{\gamma}_m \bar{\gamma}_e} \int_0^\infty \int_0^{\bar{\gamma}} e^{-\frac{\gamma_m}{\bar{\gamma}_m} - \frac{\gamma_e}{\bar{\gamma}_e}} \log_2(1 + \gamma_m) d\gamma_e d\gamma_m \\ &+ \theta \left[\frac{1}{\bar{\gamma}_m \bar{\gamma}_e} \int_0^\infty \int_0^{\bar{\gamma}} e^{-\frac{\gamma_m}{\bar{\gamma}_m} - \frac{\gamma_e}{\bar{\gamma}_e}} \log_2(1 + \gamma_m) d\gamma_e d\gamma_m \right. \\ &- \frac{2}{\bar{\gamma}_m \bar{\gamma}_e} \int_0^\infty \int_0^{\bar{\gamma}} e^{-\frac{2\gamma_m}{\bar{\gamma}_m} - \frac{\gamma_e}{\bar{\gamma}_e}} \log_2(1 + \gamma_m) d\gamma_e d\gamma_m \\ &- \frac{2}{\bar{\gamma}_m \bar{\gamma}_e} \int_0^\infty \int_0^{\bar{\gamma}} e^{-\frac{\gamma_m}{\bar{\gamma}_m} - \frac{2\gamma_e}{\bar{\gamma}_e}} \log_2(1 + \gamma_m) d\gamma_e d\gamma_m \\ &\left. + \frac{4}{\bar{\gamma}_m \bar{\gamma}_e} \int_0^\infty \int_0^{\bar{\gamma}} e^{-\frac{2\gamma_m}{\bar{\gamma}_m} - \frac{2\gamma_e}{\bar{\gamma}_e}} \log_2(1 + \gamma_m) d\gamma_e d\gamma_m \right] \end{aligned} \quad (68)$$

$$= \mathcal{W}_1 + \theta [\mathcal{W}_1 - 2\mathcal{W}_2 - 2\mathcal{W}_3 + 4\mathcal{W}_4], \quad (69)$$

where the integrals \mathcal{W}_η , for $\eta \in \{1, 2, 3, 4\}$, are in the following format [28]:

$$\int_0^\infty e^{-\zeta t} \ln(1 + t) dt = \frac{e^\zeta}{\zeta} \mathbf{E}_1(\zeta). \quad (70)$$

Thus, by exploiting (70), \mathcal{W}_η can be computed, and then the proof is completed.

Proof of $\bar{\mathcal{C}}_s^2$: By applying Lemma 2 to ASC definition in (23) and exploiting the linearity rules of integration, (23) can be decomposed as:

$$\begin{aligned} \bar{\mathcal{C}} &= \frac{1}{\bar{\gamma}_m \bar{\gamma}_e} \int_0^\infty \int_0^{\bar{\gamma}} \log_2(1 + \bar{\gamma}_{ms} + \gamma_m) e^{-\frac{\gamma_m}{\bar{\gamma}_m} - \frac{\gamma_e}{\bar{\gamma}_e}} \\ &\times \left[1 + \theta(1 - 2e^{-\frac{\gamma_m}{\bar{\gamma}_m}})(1 - 2e^{-\frac{\gamma_e}{\bar{\gamma}_e}}) \right] d\gamma_e d\gamma_m \\ &- \frac{1}{\bar{\gamma}_m \bar{\gamma}_e} \int_0^\infty \int_0^{\bar{\gamma}} \log_2(1 + \bar{\gamma}_{es} + \gamma_e) e^{-\frac{\gamma_m}{\bar{\gamma}_m} - \frac{\gamma_e}{\bar{\gamma}_e}} \\ &\times \left[1 + \theta(1 - 2e^{-\frac{\gamma_m}{\bar{\gamma}_m}})(1 - 2e^{-\frac{\gamma_e}{\bar{\gamma}_e}}) \right] d\gamma_e d\gamma_m \\ &= \mathcal{K} - \mathcal{M}, \end{aligned} \quad (71)$$

where $\bar{\gamma} = \gamma_m + \bar{\gamma}_{ms} - \bar{\gamma}_{es}$,

$$\begin{aligned} \mathcal{K} &= \frac{1}{\bar{\gamma}_m \bar{\gamma}_e} \int_0^\infty \int_0^{\bar{\gamma}} \log_2(1 + \bar{\gamma}_{ms} + \gamma_m) e^{-\frac{\gamma_m}{\bar{\gamma}_m} - \frac{\gamma_e}{\bar{\gamma}_e}} d\gamma_e d\gamma_m \\ &+ \theta \left[\frac{1}{\bar{\gamma}_m \bar{\gamma}_e} \int_0^\infty \int_0^{\bar{\gamma}} \log_2(1 + \bar{\gamma}_{ms} + \gamma_m) e^{-\frac{\gamma_m}{\bar{\gamma}_m} - \frac{\gamma_e}{\bar{\gamma}_e}} d\gamma_e d\gamma_m \right. \\ &- \frac{2}{\bar{\gamma}_m \bar{\gamma}_e} \int_0^\infty \int_0^{\bar{\gamma}} \log_2(1 + \bar{\gamma}_{ms} + \gamma_m) e^{-\frac{2\gamma_m}{\bar{\gamma}_m} - \frac{\gamma_e}{\bar{\gamma}_e}} d\gamma_e d\gamma_m \\ &- \frac{2}{\bar{\gamma}_m \bar{\gamma}_e} \int_0^\infty \int_0^{\bar{\gamma}} \log_2(1 + \bar{\gamma}_{ms} + \gamma_m) e^{-\frac{\gamma_m}{\bar{\gamma}_m} - \frac{2\gamma_e}{\bar{\gamma}_e}} d\gamma_e d\gamma_m \\ &\left. + \frac{4}{\bar{\gamma}_m \bar{\gamma}_e} \int_0^\infty \int_0^{\bar{\gamma}} \log_2(1 + \bar{\gamma}_{ms} + \gamma_m) e^{-\frac{2\gamma_m}{\bar{\gamma}_m} - \frac{2\gamma_e}{\bar{\gamma}_e}} d\gamma_e d\gamma_m \right] \quad (72) \\ &= \mathcal{K}_1 + \theta [\mathcal{K}_1 - 2\mathcal{K}_2 - 2\mathcal{K}_3 + 4\mathcal{K}_4], \quad (73) \end{aligned}$$

and

$$\begin{aligned} \mathcal{M} &= \frac{1}{\bar{\gamma}_m \bar{\gamma}_e} \int_0^\infty \int_0^{\bar{\gamma}} \log_2(1 + \bar{\gamma}_{es} + \gamma_e) e^{-\frac{\gamma_m}{\bar{\gamma}_m} - \frac{\gamma_e}{\bar{\gamma}_e}} d\gamma_e d\gamma_m \\ &+ \theta \left[\frac{1}{\bar{\gamma}_m \bar{\gamma}_e} \int_0^\infty \int_0^{\bar{\gamma}} \log_2(1 + \bar{\gamma}_{es} + \gamma_e) e^{-\frac{\gamma_m}{\bar{\gamma}_m} - \frac{\gamma_e}{\bar{\gamma}_e}} d\gamma_e d\gamma_m \right. \\ &- \frac{2}{\bar{\gamma}_m \bar{\gamma}_e} \int_0^\infty \int_0^{\bar{\gamma}} \log_2(1 + \bar{\gamma}_{es} + \gamma_e) e^{-\frac{2\gamma_m}{\bar{\gamma}_m} - \frac{\gamma_e}{\bar{\gamma}_e}} d\gamma_e d\gamma_m \\ &- \frac{2}{\bar{\gamma}_m \bar{\gamma}_e} \int_0^\infty \int_0^{\bar{\gamma}} \log_2(1 + \bar{\gamma}_{es} + \gamma_e) e^{-\frac{\gamma_m}{\bar{\gamma}_m} - \frac{2\gamma_e}{\bar{\gamma}_e}} d\gamma_e d\gamma_m \\ &\left. + \frac{4}{\bar{\gamma}_m \bar{\gamma}_e} \int_0^\infty \int_0^{\bar{\gamma}} \log_2(1 + \bar{\gamma}_{es} + \gamma_e) e^{-\frac{2\gamma_m}{\bar{\gamma}_m} - \frac{2\gamma_e}{\bar{\gamma}_e}} d\gamma_e d\gamma_m \right] \quad (74) \\ &= \mathcal{M}_1 + \theta [\mathcal{M}_1 - 2\mathcal{M}_2 - 2\mathcal{M}_3 + 4\mathcal{M}_4]. \quad (75) \end{aligned}$$

The integrals \mathcal{K}_η and \mathcal{M}_η , for $\eta \in \{1, 2, 3, 4\}$, are in the following formats [28]:

$$\begin{aligned} &\int_0^\infty e^{-\zeta t} \ln(1 + \kappa + t) dt \\ &= -\frac{1}{\zeta} \left[e^{\zeta(1+\kappa)} \mathbf{E}_1(\zeta(1 + \kappa + t)) + e^{-\zeta t} \ln(1 + \kappa + t) \right], \quad (76) \end{aligned}$$

$$\begin{aligned} &\int_0^\infty e^{-\zeta t} \ln(1 + \kappa + t) dt \\ &= \frac{1}{\zeta} \left[e^{\zeta(1+\kappa)} \mathbf{E}_1(\zeta(1 + \kappa)) + \ln(1 + \kappa) \right], \quad (77) \end{aligned}$$

$$\int_0^\infty e^{-\zeta t} \mathbf{E}_1(\delta + \nu t) dt = \frac{1}{\zeta} \left[\mathbf{E}_1(\delta) - e^{\frac{\zeta\delta}{\nu}} \mathbf{E}_1\left(\frac{\delta(\zeta + \nu)}{\nu}\right) \right]. \quad (78)$$

Therefore, by utilizing the integral formats in (76)–(78) and conducting the required simplifications, \mathcal{K} , \mathcal{M} , and then $\bar{\mathcal{C}}_s^2$ are computed.

APPENDIX D
PROOF OF THEOREM 6

First, we prove the SOP under condition of the Corollary 1. By applying Lemma 2 to (30), P_{sop}^1 can be rewritten as:

$$P_{sop}^1 = 1 - \int_0^\infty \int_{2^{R_s-1}}^\infty \frac{e^{-\frac{\gamma_m}{\bar{\gamma}_m} - \frac{\gamma_e}{\bar{\gamma}_e}}}{\bar{\gamma}_m \bar{\gamma}_e} \times \left[1 + \theta \left(1 - 2e^{-\frac{\gamma_m}{\bar{\gamma}_m}} \right) \left(1 - 2e^{-\frac{\gamma_e}{\bar{\gamma}_e}} \right) \right] d\gamma_m d\gamma_e \quad (79)$$

$$\begin{aligned} &= 1 - \left[\int_0^\infty \int_{2^{R_s-1}}^\infty \frac{e^{-\frac{\gamma_m}{\bar{\gamma}_m} - \frac{\gamma_e}{\bar{\gamma}_e}}}{\bar{\gamma}_m \bar{\gamma}_e} d\gamma_m d\gamma_e \right. \\ &+ \theta \left(\int_0^\infty \int_{2^{R_s-1}}^\infty \frac{e^{-\frac{\gamma_m}{\bar{\gamma}_m} - \frac{\gamma_e}{\bar{\gamma}_e}}}{\bar{\gamma}_m \bar{\gamma}_e} d\gamma_m d\gamma_e \right. \\ &- 2 \int_0^\infty \int_{2^{R_s-1}}^\infty \frac{e^{-\frac{2\gamma_m}{\bar{\gamma}_m} - \frac{\gamma_e}{\bar{\gamma}_e}}}{\bar{\gamma}_m \bar{\gamma}_e} d\gamma_m d\gamma_e \\ &- 2 \int_0^\infty \int_{2^{R_s-1}}^\infty \frac{e^{-\frac{\gamma_m}{\bar{\gamma}_m} - \frac{2\gamma_e}{\bar{\gamma}_e}}}{\bar{\gamma}_m \bar{\gamma}_e} d\gamma_m d\gamma_e \\ &\left. \left. + 4 \int_0^\infty \int_{2^{R_s-1}}^\infty \frac{e^{-\frac{2\gamma_m}{\bar{\gamma}_m} - \frac{2\gamma_e}{\bar{\gamma}_e}}}{\bar{\gamma}_m \bar{\gamma}_e} d\gamma_m d\gamma_e \right) \right] \quad (80) \end{aligned}$$

$$= 1 - [\mathcal{I}_1 + \theta (\mathcal{I}_1 - 2\mathcal{I}_2 - 2\mathcal{I}_3 + 4\mathcal{I}_4)], \quad (81)$$

where the integrals \mathcal{I}_η , for $\eta \in \{1, 2, 3, 4\}$ can be solved easily by performing simple calculations, and then P_{sop}^1 is obtained as (35).

Similarly, by inserting the joint PDF $f(\gamma_m, \gamma_e)$ into (33), P_{sop}^2 can be obtained as:

$$P_{sop}^2 = 1 - \int_0^\infty \int_{\gamma_{th}}^\infty \frac{e^{-\frac{\gamma_m}{\bar{\gamma}_m} - \frac{\gamma_e}{\bar{\gamma}_e}}}{\bar{\gamma}_m \bar{\gamma}_e} \times \left[1 + \theta \left(1 - 2e^{-\frac{\gamma_m}{\bar{\gamma}_m}} \right) \left(1 - 2e^{-\frac{\gamma_e}{\bar{\gamma}_e}} \right) \right] d\gamma_m d\gamma_e \quad (82)$$

$$\begin{aligned} &= 1 - \left[\int_0^\infty \int_{\gamma_{th}}^\infty \frac{e^{-\frac{\gamma_m}{\bar{\gamma}_m} - \frac{\gamma_e}{\bar{\gamma}_e}}}{\bar{\gamma}_m \bar{\gamma}_e} d\gamma_m d\gamma_e \right. \\ &+ \theta \left(\int_0^\infty \int_{\gamma_{th}}^\infty \frac{e^{-\frac{\gamma_m}{\bar{\gamma}_m} - \frac{\gamma_e}{\bar{\gamma}_e}}}{\bar{\gamma}_m \bar{\gamma}_e} d\gamma_m d\gamma_e \right. \\ &- 2 \int_0^\infty \int_{\gamma_{th}}^\infty \frac{e^{-\frac{2\gamma_m}{\bar{\gamma}_m} - \frac{\gamma_e}{\bar{\gamma}_e}}}{\bar{\gamma}_m \bar{\gamma}_e} d\gamma_m d\gamma_e \\ &- 2 \int_0^\infty \int_{\gamma_{th}}^\infty \frac{e^{-\frac{\gamma_m}{\bar{\gamma}_m} - \frac{2\gamma_e}{\bar{\gamma}_e}}}{\bar{\gamma}_m \bar{\gamma}_e} d\gamma_m d\gamma_e \\ &\left. \left. + 4 \int_0^\infty \int_{\gamma_{th}}^\infty \frac{e^{-\frac{2\gamma_m}{\bar{\gamma}_m} - \frac{2\gamma_e}{\bar{\gamma}_e}}}{\bar{\gamma}_m \bar{\gamma}_e} d\gamma_m d\gamma_e \right) \right] \quad (83) \end{aligned}$$

$$= 1 - [\mathcal{J}_1 + \theta (\mathcal{J}_1 - 2\mathcal{J}_2 - 2\mathcal{J}_3 + 4\mathcal{J}_4)], \quad (84)$$

where $\bar{\gamma}_{th} = (2^{R_s} (1 + \bar{\gamma}_{es}) - (1 + \bar{\gamma}_{ms}))$. The integrals \mathcal{J}_η , for $\eta \in \{1, 2, 3, 4\}$, can be computed by some simple calculations. Then, after conducting the required simplifications, the proof is completed.

REFERENCES

- [1] M. Matthaiou, O. Yurduseven, H. Q. Ngo, D. Morales-Jimenez, S. L. Cotton, and V. F. Fusco, "The road to 6g: Ten physical layer challenges for communications engineers," *IEEE Communications Magazine*, vol. 59, no. 1, pp. 64–69, 2021.
- [2] L. Mucchi, S. Jayousi, S. Caputo, E. Panayirci, S. Shahabuddin, J. Bechtold, I. Morales, R.-A. Stoica, G. Abreu, and H. Haas, "Physical-layer security in 6g networks," *IEEE Open Journal of the Communications Society*, vol. 2, pp. 1901–1914, 2021.
- [3] P. Porambage, G. Gür, D. P. M. Osorio, M. Liyanage, A. Gurtov, and M. Ylianttila, "The roadmap to 6g security and privacy," *IEEE Open Journal of the Communications Society*, vol. 2, pp. 1094–1122, 2021.
- [4] C. E. Shannon, "Communication theory of secrecy systems," *The Bell system technical journal*, vol. 28, no. 4, pp. 656–715, 1949.
- [5] A. D. Wyner, "The wire-tap channel," *Bell system technical journal*, vol. 54, no. 8, pp. 1355–1387, 1975.
- [6] I. Csiszár and J. Körner, "Broadcast channels with confidential messages," *IEEE transactions on information theory*, vol. 24, no. 3, pp. 339–348, 1978.
- [7] S. Leung-Yan-Cheong and M. Hellman, "The gaussian wire-tap channel," *IEEE transactions on information theory*, vol. 24, no. 4, pp. 451–456, 1978.
- [8] C. Mitropant, A. H. Vinck, and Y. Luo, "An achievable region for the gaussian wiretap channel with side information," *IEEE Transactions on Information Theory*, vol. 52, no. 5, pp. 2181–2190, 2006.
- [9] M. Costa, "Writing on dirty paper (corresp.)," *IEEE transactions on information theory*, vol. 29, no. 3, pp. 439–441, 1983.
- [10] Y. Chen and A. H. Vinck, "Wiretap channel with side information," *IEEE Transactions on Information Theory*, vol. 54, no. 1, pp. 395–402, 2008.
- [11] Y.-K. Chia and A. El Gamal, "Wiretap channel with causal state information," *IEEE Transactions on Information Theory*, vol. 58, no. 5, pp. 2838–2849, 2012.
- [12] W. Liu and B. Chen, "Wiretap channel with two-sided channel state information," in *2007 Conference Record of the Forty-First Asilomar Conference on Signals, Systems and Computers*. IEEE, 2007, pp. 893–897.
- [13] D.-S. Shiu, G. J. Foschini, M. J. Gans, and J. M. Kahn, "Fading correlation and its effect on the capacity of multielement antenna systems," *IEEE Transactions on communications*, vol. 48, no. 3, pp. 502–513, 2000.
- [14] H. Jeon, N. Kim, J. Choi, H. Lee, and J. Ha, "Bounds on secrecy capacity over correlated ergodic fading channels at high snr," *IEEE Transactions on Information Theory*, vol. 57, no. 4, pp. 1975–1983, 2011.
- [15] J. Zhu, X. Jiang, O. Takahashi, and N. Shiratori, "Effects of channel correlation on outage secrecy capacity," *Information and Media Technologies*, vol. 8, no. 4, pp. 1224–1233, 2013.
- [16] G. Pan, C. Tang, X. Zhang, T. Li, Y. Weng, and Y. Chen, "Physical-layer security over non-small-scale fading channels," *IEEE Transactions on Vehicular Technology*, vol. 65, no. 3, pp. 1326–1339, 2015.
- [17] G. C. Alexandropoulos and K. P. Peppas, "Secrecy outage analysis over correlated composite nakagami- m /gamma fading channels," *IEEE Communications Letters*, vol. 22, no. 1, pp. 77–80, 2017.
- [18] A. Mathur, Y. Ai, M. Cheffena, and G. Kaddoum, "Secrecy performance of correlated $\alpha - \mu$ fading channels," *IEEE Communications Letters*, vol. 23, no. 8, pp. 1323–1327, 2019.
- [19] F. R. Ghadi and G. A. Hodtani, "Copula-based analysis of physical layer security performances over correlated rayleigh fading channels," *IEEE Transactions on Information Forensics and Security*, vol. 16, pp. 431–440, 2020.
- [20] K.-L. Besser and E. A. Jorswieck, "Bounds on the secrecy outage probability for dependent fading channels," *IEEE Transactions on Communications*, vol. 69, no. 1, pp. 443–456, 2020.
- [21] F. R. Ghadi, G. A. Hodtani, and F. J. López-Martínez, "The role of correlation in the doubly dirty fading mac with side information at the transmitters," *IEEE Wireless Communications Letters*, vol. 10, no. 9, pp. 2070–2074, 2021.
- [22] M. H. Gholizadeh, H. Amindavar, and J. A. Ritcey, "On the capacity of mimo correlated nakagami- m fading channels using copula," *EURASIP Journal on Wireless Communications and Networking*, vol. 2015, no. 1, pp. 1–11, 2015.
- [23] S.-H. Huang, M.-N. Lo Huang, K. Thomas Wong, and T.-C. Tseng, "Copula-to model multi-channel fading by correlated but arbitrary weibull marginals, giving a closed-form outage probability of selection-combining reception," *IET Microwaves, Antennas & Propagation*, vol. 9, no. 15, pp. 1698–1705, 2015.
- [24] F. R. Ghadi and G. A. Hodtani, "Copula function-based analysis of outage probability and coverage region for wireless multiple access communications with correlated fading channels," *IET Communications*, vol. 14, no. 11, pp. 1805–1811, 2020.

- [25] C. Zheng, M. Egan, L. Clavier, G. W. Peters, and J.-M. Gorce, "Copula-based interference models for iot wireless networks," in *ICC 2019-2019 IEEE International Conference on Communications (ICC)*. IEEE, 2019, pp. 1–6.
- [26] E. A. Jorswieck and K.-L. Besser, "Copula-based bounds for multi-user communications—part i: Average performance," *IEEE Communications Letters*, vol. 25, no. 1, pp. 3–7, 2020.
- [27] R. B. Nelsen, *An introduction to copulas*. Springer Science & Business Media, 2007.
- [28] D. Zwillinger and A. Jeffrey, *Table of integrals, series, and products*. Elsevier, 2007.